On the stability of the ferromagnetic state in the Kondo-lattice compound YbNiSn under high pressure

1996 J. Phys.: Condens. Matter 8 L65

(http://iopscience.iop.org/0953-8984/8/6/001)

J. Phys.: Condens. Matter **8** (1996) L65–L70. Printed in the UK

LETTER TO THE EDITOR

On the stability of the ferromagnetic state in the Kondo-lattice compound YbNiSn under high pressure

K Drescher†, M M Abd-Elmeguid†, J P Sanchez‡ and C Meyer§

† II. Physikalisches Institut, Universität zu Köln, Zülpicher Strasse 77, 50937 Köln, Germany
‡ Département de Recherche Fondamentale sur la Matière Condensée, CEA/Grenoble, 17 rue des Martyrs, 38054 Grenoble Cédex 9, France
§ Laboratoire Louis Néel, Centre National de la Recherche Scientifique, BP 166, 38042 Grenoble Cédex 9, France

Received 25 November 1995

Abstract. The effect of pressure on the electrical resistance $R(T, p)$ (where $p \leqslant 13$ GPa and 1.8 K $\leqslant T < 300$ K) and the lattice parameters ($p \leqslant 26.4$ GPa at $T = 300$ K) of the ferromagnetic Kondo-lattice compound YbNiSn ($T_C = 5.5$ K at ambient pressure) has been investigated using the diamond anvil cell technique. The x-ray diffraction data show a smooth decrease of the lattice parameters upon increasing pressure, indicating no structural phase transition up to 26.4 GPa. $R(T, p)$ measurements show for $0 \leqslant p \leqslant 9$ GPa the same pressure dependence of T_C as obtained from very recent high-pressure ac susceptibility ($\chi_{ac}(p)$) measurements. However, unlike for the $\chi_{ac}(p)$ measurements, where the ferromagnetic signal is lost for pressures $p \geqslant 9.4$ GPa, we find an almost pressure-independent value of T_C in the pressure range $6 \leqslant p \leqslant 13$ GPa, i.e. no indication of a discontinuous change of the type of magnetic order is observed at $p = 9.4$ GPa. We further discuss the correlation between the pressure dependence of T_C and that of the characteristic temperature of crystal-electric-field effects T^*_{CEF}.

The rare-earth (R) ternary intermetallic compounds RNiSn which crystallize in the orthorhombic ϵ-TiNiSi-type [1] structure show a variety of interesting magnetic properties depending on the choice of R [2]. Among these compounds YbNiSn has recently attracted considerable interest as being a ferromagnetic (FM) ($T_C \approx 5.5$ K) Kondo-lattice (KL) system which exhibits features of heavy-fermion systems [3, 4, 5]. At high temperatures the magnetic susceptibility reveals Curie–Weiss behaviour with an effective moment of $\mu_{eff} \approx 4.3\ \mu_B$ [3], which is close to the value for the free Yb^{3+} ion ($\mu_{eff} = 4.54\ \mu_B$). Below T_C, the Yb^{3+} magnetic moments lie along the c-axis with a saturated value of $\mu_S = 0.85\mu_B$ [5], which is lower than that expected from the analysis of the paramagnetic state ($1.1\mu_B$ [5]) made by considering the influence of the crystal electric field (CEF). The reduction of μ_S is suggested to be caused by the hybridization of the localized 4f electrons with the conduction electrons [3, 5]. The relatively high electronic specific heat coefficient ($\gamma \approx 300$ mJ K^{-2} mol^{-1} at low temperatures [4]) for YbNiSn supports the coexistence of the magnetic order with a heavy-electron state.

In this respect, high-pressure studies on KL systems are of particular interest because the ground-state properties of these systems are expected to be sensitive to external pressure (p) [6]. This is related to the fact that p modifies the strength of the exchange interaction J between localized 4f electrons and conduction electrons and thereby the competition between the intersite (RKKY) and intrasite (Kondo) interactions with the characteristic temperatures

0953-8984/96/060065+06$19.50

T_{RKKY} and T_K, respectively. This delicate balance is described theoretically by Doniach [7] for a magnetic phase diagram depending on J.

Experimentally, recent measurements of the electrical resistivity of YbNiSn under pressure ($0 \leqslant p \leqslant 1.7$ GPa) [8] revealed a gradual increase of T_C from 5.5 K at ambient pressure to 7.6 K at 1.7 GPa. This result was discussed within the Doniach model as a decrease in J with increasing p, which reduces the Kondo spin compensation and thereby favours long-range magnetic order. Actually, $T_K \propto \exp(-1/|J|)$ and $T_{RKKY} \propto J^2$, $\sim$0.7 K and $\sim$7.3 K, respectively, at ambient pressure [9], decrease with pressure. However, the exponential fall of T_K is much more dramatic than that of T_{RKKY}. Very recent high-pressure ac susceptibility ($\chi_{ac}(p)$) measurements on YbNiSn over an extended pressure range $0 \leqslant p \leqslant 38$ GPa [10] reveal that the enhanced T_C passes through a maximum at about $p \approx 2$ GPa and then falls to $T_C \approx 5.3$ K for $6 < p \leqslant 9.4$ GPa. This result provides the first qualitative experimental confirmation of the Doniach model in a magnetically ordered Yb Kondo-lattice compound. However, it is found that T_C is almost pressure independent in the pressure range $6 \leqslant p \leqslant 9.4$ GPa which is notably different to what is found for Ce compounds [11, 12]. In addition, the authors of [10] show another interesting finding, namely the disappearance of the ferromagnetic signal for $p \geqslant 9.4$ GPa. This was suggested to be related to a transition from the ferromagnetic to an antiferromagnetic or nonmagnetic state, which might be accompanied by a structural phase transition.

In order to obtain a deeper insight into the stability of the ferromagnetic state of YbNiSn under high pressure, we have performed measurements of the electrical resistance ($R(T, p)$) at pressures in the range $0 \leqslant p \leqslant 13$ GPa and for the temperature range $1.8\ \mathrm{K} \leqslant T \leqslant 300$ K. Measurements of $R(T, p)$ allow one not only to determine the pressure-induced change of T_C but also to study corresponding variations of the CEF and electron correlation effects which are known to be important for the ground-state properties of YbNiSn [5]. We have also performed x-ray diffraction measurements under pressures in the range $0 \leqslant p \leqslant 26.4$ GPa and at 300 K in order to investigate the structural stability of YbNiSn under high pressure, particularly in the pressure range around $p = 9.4$ GPa, where the ferromagnetic signal of $\chi_{ac}(p)$ measurements is lost [10].

Polycrystalline YbNiSn was prepared by melting stoichiometric amounts of the constituents in a sealed molybdenum crucible and by post-annealing the sample at 800 $^\circ$C for several days.

Measurements of the electrical resistance have been performed using the diamond anvil cell technique [13, 14]. We have used a dc four-probe technique, where the current direction was automatically reversed to eliminate thermovoltages. Pressure was determined by measuring the pressure-induced shift of the R_1 fluorescence line of ruby.

The pressure-dependent variation of the lattice constants was measured at the energy-dispersive x-ray diffraction station for high pressure at LURE in Paris. Measurements were performed using the diamond anvil cell technique with silicon oil as the pressure-transmitting medium.

Figure 1 shows the pressure dependence of the lattice parameters for pressures $0 \leqslant p \leqslant 26.4$ GPa at 300 K and figure 2 displays the pressure dependence of the relative volume in the same pressure range. A smooth decrease of all lattice parameters is observed upon increasing the pressure. There is no evidence for any structural phase transition up to 26.4 GPa. Experimental data points in figure 2 have been fitted to Murnaghan's equation of state using $V_0 = 233.5$ Å^3, $B_0 = 146(20)$ GPa and $B_0' \approx 2.6$. The value of B_0 is comparable to results for related Yb compounds [15].

Figure 3 displays the electrical resistance $R(T, p)$ in the temperature range $1.8\ \mathrm{K} \leqslant T \leqslant 300$ K for pressures in the range $0 \leqslant p \leqslant 13$ GPa. For a better comparison the curves

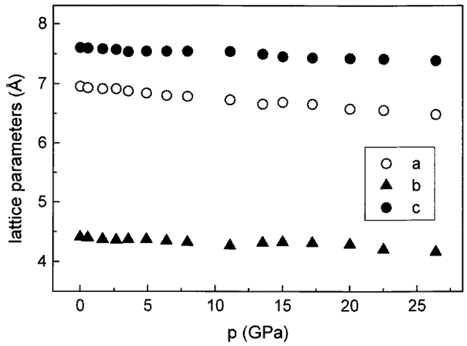

Figure 1. The pressure dependence of the lattice parameters a (○), b (▲) and c (●) of YbNiSn (orthorhombic structure, space group *Pnma*).

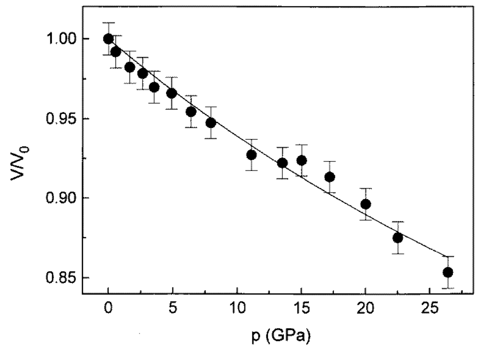

Figure 2. The pressure variation of the relative volume V/V_0 of YbNiSn. The solid line is a fit to Murnaghan's equation of state (see the text).

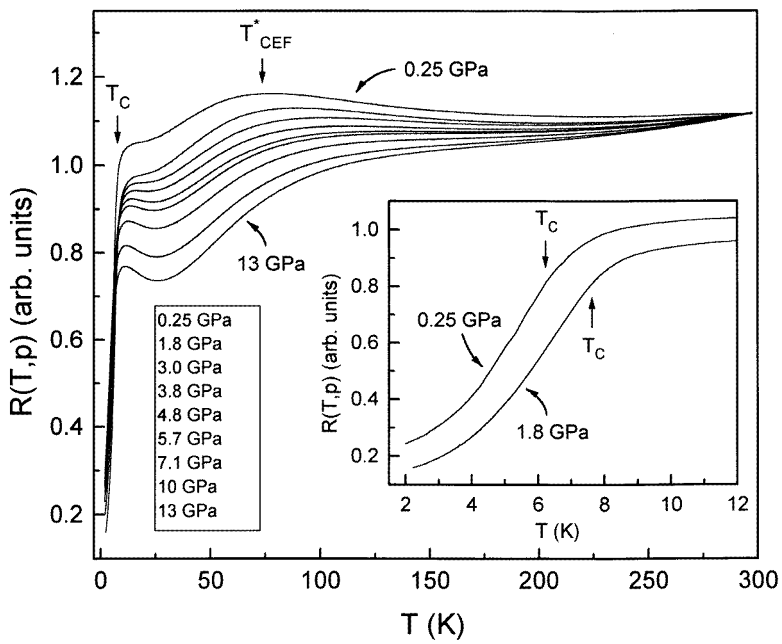

Figure 3. The electrical resistance $R(T, p)$ of YbNiSn at different pressure points and as a function of temperature. Pressure values corresponding to $R(T, p)$ curves are given in the figure. The inset shows $R(T, p)$ for the temperature range $2 \leqslant T \leqslant 12$ K and at pressures of 0.25 GPa and 1.8 GPa.

were shifted along the $R(T, p)$ axis so as to have the same starting point at 295 K. Since we are not able to measure absolute values of the resistance, $R(T, p)$ is given in arbitrary units.

As is evident from figure 3, $R(T, p)$ shows a double-peak structure as reported previously [4, 8]. These features have been attributed to Kondo-lattice behaviour. The maximum that appears at higher temperatures is attributed to CEF population effects (e.g. $T^*_{CEF} \approx 80$ K at $p = 0.25$ GPa) [16]. At low temperatures $10 \text{ K} \leqslant T \leqslant 30$ K, the resistance develops a shoulder, which is followed by a drop of the resistance for the onset of ferromagnetic order (T_C). The value of the resistance for $T < T_C$ is an order of magnitude smaller than that for $T > 10$ K.

The maximum at around 100 K (CEF) can clearly be seen for pressures $p \leqslant 5.7$ GPa. The slope of $R(T)$ for temperatures in the range $10\ \text{K} \leqslant T \leqslant 25$ K which is small but positive at $p = 0.25$ GPa decreases with increasing pressure until it becomes clearly negative for pressures above $p = 4.8$ GPa. Over the whole pressure range ($0 \leqslant p \leqslant 13$ GPa) YbNiSn reveals a KL behaviour.

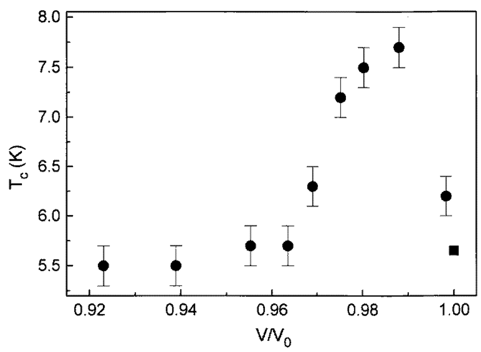

Figure 4. The magnetic ordering temperature T_C of YbNiSn as a function of relative volume V/V_0. The datum point at ambient pressure (filled square) is taken from [8].

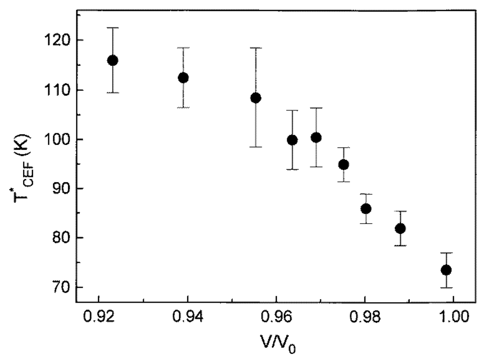

Figure 5. The volume dependence of the characteristic temperature of crystal-electric-field effects T^*_{CEF} for YbNiSn. T^*_{CEF} is defined in the text.

T_C is defined as the temperature where $\mathrm{d}^2R/\mathrm{d}T^2$ shows an extremum. Using this definition, we have plotted the values of T_C as a function of relative volume in figure 4. The values for $p \leqslant 9.4$ GPa are in good agreement with very recent $\chi_{ac}(p)$ measurements [10]. On the other hand the characteristic temperature for crystal-field effects was determined using $T^*_{CEF} = (T_1 + T_2)/2$, where T_1 is the temperature where $\mathrm{d}R/\mathrm{d}T$ has a maximum and T_2 is the temperature where $\mathrm{d}R/\mathrm{d}T$ has a minimum in the temperature range $25\ \text{K} < T < 300$ K. In this way, T^*_{CEF} is defined even in the pressure range where no explicit maximum can be found. The values of T^*_{CEF} obtained for pressures $p \leqslant 1.8$ GPa are in good agreement with previous measurements [8]. The estimated values of T^*_{CEF} as a function of volume are plotted in figure 5.

In the following we first discuss the volume dependence of T_C which is shown in figure 4. As mentioned above, we find a good agreement with $\chi_{ac}(p)$ data [10] in the pressure range $p \leqslant 9.4$ GPa. However, we still observe the same features of the $R(T, p)$ curves, particularly the resistance drop at low temperatures for pressures $p > 9.4$ GPa. This finding suggests that long-range magnetic order still *exists* in this pressure range ($9.4\ \text{GPa} \leqslant p \leqslant 13$ GPa), so a transition to a nonmagnetic state can be excluded. As is evident from figure 4 one can distinguish between two regions in which T_C exhibits completely different volume dependences: there is a large variation in T_C for $V/V_0 \geqslant 0.96$. Here one finds a sharp increase of T_C from 5.5 K to 7.7 K at $V/V_0 \approx 0.99$ followed by a drop of T_C to 5.7 K at $V/V_0 \approx 0.96$, a value which is close to the value at ambient pressure. It is to be noticed that such a large initial change of T_C with p implies a rather large magnetic Grüneisen parameter $\Omega_M(p \to 0) = -\partial \ln T_C/\partial \ln V \approx +40$, which is suggested to be a precursor effect of a subsequent change of the magnetic structure at high pressures [17].

In the second region, $0.96 \geqslant V/V_0 \geqslant 0.92$, one finds that T_C is hardly affected by decreasing volume and no anomaly in T_C is observed at $p = 9.4$ GPa. This result seems to contradict that obtained from $\chi_{ac}(p)$ measurements, where the ferromagnetic signal is lost at $p = 9.4$ GPa [10]. There are two possibilities for explaining our observation in this pressure range: (i) T_C may be not sensitive to the change in the type of magnetic order; or (ii) the pressure-induced change of the spin structure may be gradual.

Since the magnetic ordering temperature of local moment systems is sensitive to any change of the spin structure [17], we believe that the change of the spin structure should be gradual, e.g. from a collinear FM structure to a complex type of magnetic order with a vanishing ferromagnetic component for pressures above 9.4 GPa.

In this connection, we want to discuss another interesting aspect of our study, namely the influence of pressure on CEF effects in YbNiSn and its possible relationship to the pressure dependence of T_C. As mentioned above, the maximum in the resistance at around 100 K can be attributed to CEF effects. The pressure dependence of T^*_{CEF} can be seen in figure 5. We find a large linear rate of increase of T^*_{CEF} with decreasing volume for $V/V_0 \geqslant 0.96$ and a smaller one for $V/V_0 < 0.96$. If one compares the volume dependence of T_C and T^*_{CEF}, a correlation of the behaviour of these two characteristic temperatures can be found. Both quantities are sensitive to volume changes for $V/V_0 \geqslant 0.96$ and almost volume independent for $0.96 > V/V_0 > 0.92$. This correlation leads to the assumption that one has to consider CEF effects to explain the pressure-induced changes of the magnetic properties of YbNiSn. It is worth mentioning here that the actual moment direction in YbNiSn results from the competition between the CEF anisotropy which favours a moment orientation along the *a*-axis and the anisotropic exchange interaction which tends to align the moments along the *c*-axis [5]. As known for some Ce KL compounds, the simultaneous occurrence of CEF effects and Kondo-like coupling can lead to complex magnetic structures, e.g. with modulated moments, even for a ground-state Kramers doublet [17]. In Ce compounds pressure reduces T^*_{CEF} and a transition from a complex magnetic order to a collinear order can be observed. In contrast to this, in Yb compounds T^*_{CEF} is enhanced by pressure and one would expect (in analogy to the case for Ce compounds) a transition from a collinear (here ferromagnetic) order to a more complex magnetic order. In this respect we want to refer to the similarity between the resistance curves of YbNiSn for pressures above 6 GPa and that of the isostructural compound YbPtAl [18]. YbPtAl orders antiferromagnetically below $T_N = 5.8$ K and shows metamagnetic behaviour in a rather low (0.5 T) magnetic field [18]. This again would give further support for our suggestion of a pressure-induced complex magnetic structure in YbNiSn.

In summary, our x-ray diffraction data obtained under high pressure reveal that the crystal structure of YbNiSn is stable up to pressures of 26.4 GPa. On the other hand, we have shown from measurements of the electrical resistance at high pressures that the anomalous pressure dependence of T_C is related to a pressure-induced instability of the ferromagnetic state of YbNiSn. The observed strong correlation of the pressure dependence of T_C and T^*_{CEF} leads to the conclusion that CEF effects have to be considered in explaining the effect of pressure on the magnetic properties of YbNiSn. It would be of great interest to investigate the stability of the magnetic structure of YbNiSn under high pressure using direct experimental methods, e.g. neutron diffraction or ^{170}Yb Mössbauer effect methods. Such experiments are under way in our laboratory.

It is a pleasure to acknowledge J P Itié and A Polian for their assistance at LURE and enlightening advice. We are also grateful to J A Hodges for providing the YbNiSn sample and to H Micklitz and J S Schilling for useful discussions.

References

[1] Dwight A E 1983 *J. Less-Common Met.* **93** 411
[2] Skolozdre R V, Loretskaya O E and Gorelenko Yu K 1984 *Inorg. Mater.* **20** 604
[3] Kasaya M, Tani T, Iga F and Kasuya T 1988 *J. Magn. Magn. Mater.* **76 + 77** 278
[4] Kasaya M, Tani T, Kawate K, Mizushima T, Isikawa Y and Sato K 1991 *J. Phys. Soc. Japan* **60** 3145
[5] Bonville P, Bellot P, Hodges J A, Imbert P, Jehanno G, LeBras G, Hammann J, Leylekian L, Cherrier G, Thuery P, D'Onforio L, Hamzic A and Barthelemy A 1992 *Physica* B **182** 105
[6] Thompson J D and Lawrence J L 1994 *Handbook on the Physics and Chemistry of Rare Earths* ed K A Gschneidner, L Eyring Jr, G H Lander and G R Cloppin (Amsterdam: North-Holland) p 383
[7] Doniach S 1977 *Physica* B **91** 231
[8] Sparn G, Thompson J D and Hamzić A 1992 *J. Alloys Compounds* **181** 197
[9] Bonville P, Polatsek G, Hodges J A, Imbert P and LeBras G 1993 *Physica* B **186–188** 254
[10] Cornelius A L, Schilling J S, Mandrus D and Thompson J D 1996 *Phys. Rev.* B at press
[11] Cornelius A L and Schilling J S 1994 *Phys. Rev.* B **49** 3955
[12] Malik S K, Shenoy G K, Dhar S K, Paulose P L and Vijayaragharan R 1986 *Phys. Rev.* B **34** 8196
[13] van Eenige E N, Griessen R and Wijngaarden R J 1990 *Physica* C **168** 482
[14] Drescher K and Abd-Elmeguid M M 1994 *Physica* B **206+207** 14
[15] Bauer E, Hauser R, Gratz E, Payer K, Oomi G and Kagayama T 1993 *Phys. Rev.* B **48** 15 873
[16] Cornut B and Coqblin B 1972 *Phys. Rev.* B **5** 4541
[17] Morin P, Vettier C, Flouquet J, Konczykowski M, Lassaily Y, Mignot J M and Welp U 1988 *J. Low Temp. Phys.* **70** 377 and references therein
[18] Diehl J, Davideit H, Klimm S, Tegel U, Geibel C, Steglich F and Horn S 1995 *Physica* B **206 + 207** 344